Thio-glucose bound gold nanoparticles enhance radio-cytotoxic targeting of ovarian cancer

2011 Nanotechnology 22 285101

(http://iopscience.iop.org/0957-4484/22/28/285101)

Nanotechnology **22** (2011) 285101 (8pp) doi:10.1088/0957-4484/22/28/285101

Thio-glucose bound gold nanoparticles enhance radio-cytotoxic targeting of ovarian cancer

Feng Geng[1,8], Kun Song[1,8], James Z Xing[2,3], Cunzhong Yuan[1], Shi Yan[1], Qifeng Yang[4], Jie Chen[5,6,7] and Beihua Kong[1,9]

[1] Department of Obstetrics and Gynecology, Qilu Hospital, Shandong University, Jinan, People's Republic of China
[2] Department of Radiation Oncology, Cross Cancer Institute, Edmonton, AB, Canada
[3] Department of Laboratory Medicine and Pathology, University of Alberta, Edmonton, AB, Canada
[4] Department of Breast Surgery, Qilu Hospital, Shandong University, Jinan, People's Republic of China
[5] Department of Biomedical Engineering, University of Alberta, Edmonton, AB, Canada
[6] Department of Electrical and Computer Engineering, University of Alberta, Edmonton, AB, Canada
[7] National Institute for Nanotechnology, Edmonton, AB, Canada

E-mail: kongbeihua@yahoo.com.cn

Received 12 February 2011, in final form 19 April 2011
Published 8 June 2011
Online at stacks.iop.org/Nano/22/285101

Abstract
The treatment of ovarian cancer has traditionally been intractable, and required novel approaches to improve therapeutic efficiency. This paper reports that thio-glucose bound gold nanoparticles (Glu-GNPs) can be used as a sensitizer to enhance ovarian cancer radiotherapy. The human ovarian cancer cells, SK-OV-3, were treated by gold nanoparticles (GNPs) alone, irradiation alone, or GNPs in addition to irradiation. Cell uptake was assayed using inductively coupled plasma atomic emission spectroscopy (ICP-AES), while cytotoxicity induced by radiotherapy was measured using both 3-(4,5)-dimethylthiahiazo (-z-y1)-3,5-di-phenytetrazoliumromide and clonogenic assays. The presence of reactive oxygen species (ROS) was determined using CM-H2-DCFDA confocal microscopy and cell apoptosis was determined by an Annexin V-FITC/propidium iodide (PI) kit with flow cytometry. The cells treated by Glu-GNPs resulted in an approximate 31% increase in nanoparticle uptake compared to naked GNPs ($p < 0.005$). Compared to the irradiation alone treatment, the intracellular uptake of Glu-GNPs resulted in increased inhibition of cell proliferation by 30.48% for 90 kVp and 26.88% for 6 MV irradiation. The interaction of x-ray radiation with GNPs induced elevated levels of ROS production, which is one of the mechanisms by which GNPs can enhance radiotherapy on ovarian cancer.

S Online supplementary data available from stacks.iop.org/Nano/22/285101/mmedia

(Some figures in this article are in colour only in the electronic version)

1. Introduction

Ovarian cancer is particularly insidious in nature and is the leading cause of death among gynecological malignancies [1]. In 2009, 21 550 new cases were diagnosed and 14 600 women died of ovarian cancer in the United States alone. Only 20% of patients are diagnosed early enough for treatment to be effective [2]. Traditional methods of chemotherapy, surgery, and radiotherapy can control cancer symptoms; however, these procedures lack targeting specificity [3]. In particular, radiotherapy covers all cancer cells within its

[8] These authors equally contributed to this article.
[9] Address for correspondence: Department of Obstetrics and Gynecology, Qilu Hospital of Shandong University, 107 Wenhuaxi Road, Jinan, 250012, Shandong, People's Republic of China

radiation field, inevitably subjecting abdominal organs, such as the liver, kidneys, and small bowel, to lethal radiation. For radiotherapy to be effective, a therapeutic mechanism is needed in order to enhance the cancer killing effects while minimizing cytotoxicity to surrounding tissues. Current data provide insight on gold nanoparticle (GNP) enhanced radiation therapy on ovarian cancer cells.

Previous studies using metallic nanoparticles show promising tumor-killing potential over conventional methods of chemotherapy, radiation, or surgery [4]. Gold is an ideal material that ensures biocompatibility while being capable of forming reactive oxygen species when irradiated [5–11]. Using 1.9 nm GNPs, Hainfeld *et al* [12] obtained dose enhancement ratios of at least two when tumor bearing mice were irradiated with 250 kVp x-rays. Our previous research has shown that Glu-GNPs significantly increased cell uptake by various types of cancer tissues compared to bare nanoparticles [12, 13]. Glu-GNPs showed a 1.5–2.0 fold enhancement in growth inhibition compared to GNPs alone in prostate and breast cancer treatment [12]. Its effect on ovarian cancer remains to be investigated. In this paper, we investigate Glu-GNPs enhanced target cytotoxicity of radiation on ovarian cancer cells.

2. Materials and methods

2.1. Chemicals

Gold (III) chloride trihydrate ($HAuCl_4{\cdot}3H_2O$, G4022-1g), sodium borohydride ($NaBH_4$, 452882), sodium citrate iribasic dehydrate ($C_6H_5Na_3O_7{\cdot}2H_2O$, S4641-500G), 1-thio-D-glucose (GLU, T6375-1G) and polyethylene glycol (PEG 5000, 11124) were purchased from Sigma-Aldrich, USA. All the materials were dissolved in deionized water purified by the Milli-*Q* Biocel system (ZMQS50F01, Millipore, USA).

2.2. Synthesis of GNPs

Three sub-steps were involved in GNP synthesis. (i) 3.2 ml of 25 mM $HAuCl_4$ solution was added to 60 ml of deionized water in an ice bath under moderate stirring. (ii) 4 ml of 26 mM $NaBH_4$ was then added as a reducing agent to obtain naked GNPs. (iii) 22.4 ml of naked GNP solution was added to two tubes: the first containing 4 ml of 20 mM 1-thio-β-glucose and the second containing 4 ml of 38.8 mM sodium citrate solution. Thio-glucose formed a covalent bond with the GNPs while sodium citrate was electrostatically bound to the GNPs to form functionalized Glu-GNPs and neutral naked GNPs, respectively. Both the naked GNPs and the Glu-GNPs were dialyzed for two days to remove any free sodium citrate or thio-glucose before these solutions were used for the experiments.

The gold (Au) concentration was tested by inductively coupled plasma atomic emission spectroscopy (ICP-AES) (IRIS INTREPID II XSP). The morphology of gold nanoparticles was characterized using transmission electron microscopy (TEM) (JEM-100CX, Japan). The size distribution of GNPs was determined by dynamic light scattering (DLS) (LB-550, HORIBA Jobin Yvon, USA). X-ray photoelectron spectroscopy (XPS) (ESCALAB 250, Thermo Fisher scientific, USA) was used for surface characterization of Glu-GNPs to determine the elemental composition of each Glu-GNP.

2.3. Cell lines and culture conditions

SK-OV-3 (HTB-77), an epithelial ovarian cancer cell line, was purchased from American Type Culture Collection (ATCC) and cultured in RPMI Medium 1640 (GIBCO, Invitrogen Corporation) supplemented with 10% heat-inactivated fetal bovine serum (FBS, GIBCO). Cells were cultured in water jacketed CO_2 incubators (Thermo Fisher Scientific Forma® Series II, USA) at 37 °C with 95% (v/v) air and 5% (v/v) CO_2 in a humidified atmosphere.

2.4. Cell uptake of GNPs and Glu-GNPs

SK-OV-3 cell were cultured in 6 cm dishes. When the cells reached 70% confluence, GNPs and Glu-GNPs were added into the medium respectively for a final concentration of 5 nM. Because FBS might have an impact on binding and internalization of GNPs, we used FBS-free medium when GNPs were incubated with the cells. In brief, we removed the culture medium containing FBS and washed the cells with PBS buffer twice. The cells were then cultured with FBS-free medium and treated with GNPs. After the treatment, the medium containing FBS was used to replace FBS-free medium. After incubation at different intervals (1, 2, 4, 8, 12, 24, 48, and 96 h), the cells were collected and then re-suspended into PBS for a final volume of 5 ml. The number of cells was counted using a hemocytometer. 5 ml of 20% HNO_3 was added into each sample to lyse the cells. The gold mass in the lysis solution was measured by ICP-AES. The number of GNPs was calculated via the gold mass, and the number of GNPs in the lysis solution divided by the number of cells provided a quantitative measurement of GNP cell uptake.

2.5. Irradiation and cell survival assay

SK-OV-3 ovarian cancer cells were seeded at approximately 2×10^3 per well of a 96-well tissue culture plate and incubated overnight. The medium was replaced by fresh medium containing different concentrations of Glu-GNPs (0, 1, and 5 nM). 24 h later, the medium containing GNPs was removed, the cells were washed twice with PBS, and new medium with FBS was added. The cells were then divided into two groups, one without irradiation, and the other was followed by either (i) irradiation with low-energy 90 kVp x-rays (Faxitron x-rays); or (ii) irradiation with high-energy 6 MV photons, by a medical linear accelerator (Varian 23EX linear accelerator, USA), each with a total dose of 10 Gy. After irradiation, cells were incubated at different intervals (24, 48, 72, and 96 h, respectively). The cells without nanoparticles or irradiation served as controls. For all experiments, cell viability was measured using the 3-(4,5)-dimethylthiahiazo (-z-y1)-3,5-di-phenytetrazoliumromide (MTT) (Amresco, 0793-1G) assay. The results for cellular survival in response to Glu-GNPs with and without radiation were determined using the Opsys MR™ 96-well microplate reader (CB372, DYNEX, USA) and expressed as the absorbance at 490 nm at the indicated points in time.

2.6. Analysis of cell colony formation

For the clonogenic survival assay, both sets of cells, with or without treatment, were incubated for two weeks. Cells were then fixed with 3:1 ethanol to acetic acid solution and stained with crystal violet. Colonies were counted for the control and experimental groups, with each experiment performed in triplicate.

2.7. Determination of intracellular reactive oxygen species (ROS) concentration

Measurement of intracellular ROS concentration is described in the literature [14]. In brief, SK-OV-3 cells growing on 40 mm diameter glass cover slips were incubated with buffer containing 10 μM dichlorodihydrofluorescein diacetate (DCFH-DA). After incubation for 20 min at 37 °C, cells were washed three times with phosphate-buffered saline (PBS), and the change of intracellular ROS was detected by scanning fluorescence intensity under confocal microscopy (Leica TCS SP2). The images were quantitatively treated with the software ImageJ (NIH, USA). The three-dimensional (3D) surface plots were obtained and then the peaks' volume was calculated after background subtraction and the cell area was also calculated. The mean intensity of fluoresce area was defined as a peak volume/cell area and then normalized with the control image.

2.8. Cell apoptosis determined by flow cytometry (FCM)

SK-OV-3 cell apoptosis was analyzed using an Annexin V-FITC Apoptosis Detection kit I (BD pharmingen™, cat No. 556547) according to the manufacturer's protocol. In brief, harvested cells were re-suspended in 100 μl binding buffer and adjusted to about 1×10^5 ml^{-1}. After 5 μl Annexin V-FITC and 5 μl PI (20 μg ml^{-1}) were added, the cells were incubated for 15 min at room temperature in the dark, then another 400 μl binding buffer was added. Flow cytometry was conducted on a FACS caliber (BD Biosciences, Hercules, CA, USA).

2.9. Flow cytometry analysis of cell cycle

The cells fixed in 70% ethanol were washed, re-suspended, and treated with 10 μg ml^{-1} RNase for 30 min at 37 °C, and then stained with PBS containing 50 μg ml^{-1} PI for 30 min at 4 °C. Analysis was performed with a FACSCalibur flow cytometer (BD Biosciences, Hercules, CA, USA). These tests were performed in triplicate and each 20 000 cell sample was tested. Values were expressed as the mean ± standard deviation (SD).

2.10. Statistical analysis

Experimental values were determined in triplicate. All values involving gold content are expressed as means and standard errors (SE). The one-way analysis of variance (ANOVA) and Tukey multiple comparison post-test were used. Differences less than 0.05 ($p < 0.05$) were considered statistically significant.

3. Results

3.1. Characterization of GNPs

The average gold concentration of the GNP solutions synthesized was 80 mg l^{-1}, measured by ICP-AES. Figure 1(A) shows the TEM image of GNPs. Thio-glucose (figure 1(B)) was capped onto the surface of GNPs to form Glu-GNPs (figure 1(C)). Figure 1(D) shows the size distribution of GNPs measured by DLS. The actual diameter of the GNPs was 14.37 ± 2.49 nm, calculated based on measurements made by TEM. The GNPs used in the study had the same size. The average number of biomolecules (approximately 2.5×10^4 thio-glucose) on one nanoparticle was calculated by measuring the gold-to-sulfur atom ratio acquired with XPS.

3.2. Distributions and uptakes of GNPs and Glu-GNPs

SK-OV-3 cells were incubated with 5 nM GNPs and 5 nM Glu-GNPs, respectively. Figure 2(A) shows the average number of nanoparticles internalized by each cell at individual time points (1–96 h). It illustrates that the uptake of both GNPs and Glu-GNPs by SK-OV-3 cells increased with incubation time during the first 48 h. Peak uptake concentration for both naked GNPs and Glu-GNPs was observed at 48 h. SK-OV-3 cells internalized much more Glu-GNPs than naked GNPs at each interval of time. After treatment with the nanoparticles for 4 h, the average numbers of the nanoparticle internalized by each cell was $(8.00 \pm 0.90) \times 10^3$ for naked GNPs and $(9.30 \pm 0.68) \times 10^3$ for Glu-GNPs, respectively ($P = 0.026$).

3.3. Cytotoxicity of GNPs and Glu-GNPs

5 nM of either GNPs or Glu-GNPs were incubated with cells separately and the cytotoxicity of the nanoparticles without radiation was measured by an MTT test. Cell survival rates after 48–96 h treatment were determined by an MTT assay. Figure 2(B) shows three groups with 0, 1, and 5 nM Glu-GNPs without x-ray radiation. Cell viability for groups with 1 nM and 5 nM Glu-GNPs were 96.8% and 96.8% respectively on day 2 ($P > 0.05$), 97.3% and 93.2% on day 4 ($P > 0.05$), compared to the control group without Glu-GNPs (figure 2(B)). These results in cell survival analysis indicate that Glu-GNPs in either 1 or 5 nM concentrations did not induce remarkable cytotoxicity on SK-OV-3 cells.

3.4. Glu-GNPs enhanced radiation sensitivity of SK-OV-3 cells

Figures 2(C) and (D) show that Glu-GNPs enhanced radiation sensitivity of SK-OV-3 cells. No significant differences were observed between groups receiving 6 MV or 90 kVp irradiation ($P > 0.05$). Glu-GNPs subject to x-ray radiation reduced the survival rate remarkably compared to groups treated with x-ray radiation alone. For example, 90 kVp irradiation alone (5 Gy) induced a survival rate of 64.39% for SK-OV-3 cells while Glu-GNPs (5 nM) enhanced the radio-sensitivity, thus reducing the cell survival rate to 44.76% (figure 2(C)). The 1.25, 2.5, and 5 nM Glu-GNPs enhanced the cell sensitivities

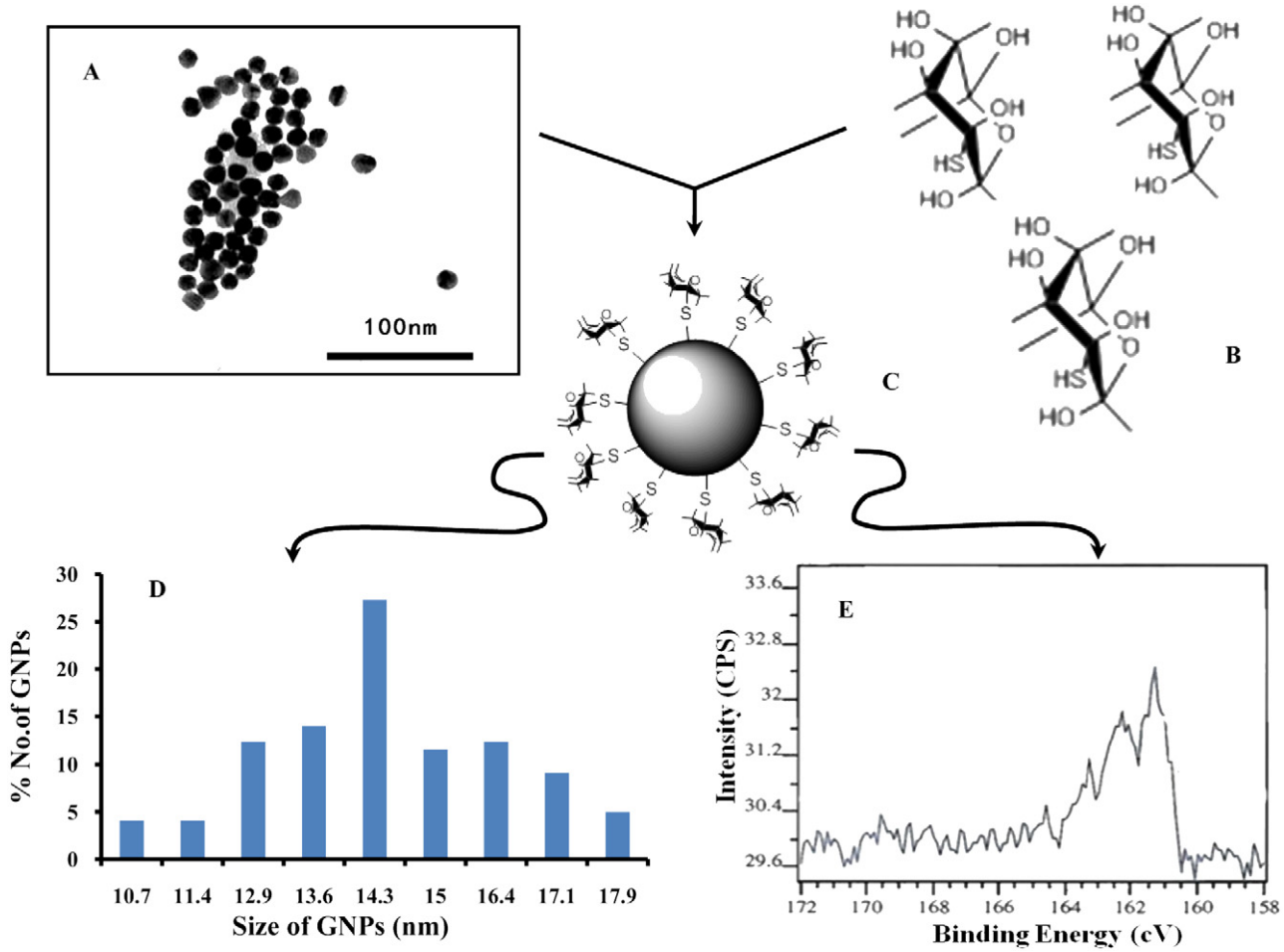

Figure 1. Characterizing Glu-GNPs. (A) TEM picture of GNPs alone; (B) and (C) the schematic of GNPs coated with thio-glucose; (D) the size distribution of Glu-GNPs measured by DLS; (E) characterizing Glu-GNPs using XPS.

toward 5 Gy 6 MV irradiation, showing survival rates ranging from 79.6% for x-ray alone to 61.3%, 60.0%, and 58.2% for the combined treatments, respectively. A significant decrease in survival rate was observed, averaging 10.6% ($P < 0.01$) compared to controls (figure 2(D)).

Cell colony formation assay was also used to determine the sensitivity of Glu-GNPs enhanced radiation. 6 MV irradiation with doses of 2.5, 5, 10, 15, and 20 Gy induced inhibitory rates of 9.9%, 26.1%, 39.6%, 56.8%, and 76.2%, respectively. If 5 nM Glu-GNPs were added before irradiation, the same doses of irradiation produced inhibitory rates of 11.7%, 30.6%, 61.4%, 92.8%, and 100%, respectively ($P < 0.007$) (figure 2(F)). Similar enhancement ratios were observed for 90 kVp irradiation groups. Cells subject to 90 kVp radiation doses of 2.5, 5, 10, 15, and 20 Gy experienced growth inhibition rates of 17.7%, 35.6%, 54.5%, 78.6%, and 95.5%, respectively. When combined with 5 nM Glu-GNPs, the same dose of radiation-induced cellular inhibitory rates were found with 26.2%, 55.2%, 91.7%, 100%, and 100%, respectively ($P < 0.007$) (figure 2(E)). A comparison of enhancement rates induced by either 6 MV or 90 kVp irradiations is shown in figure 2(G). Higher sensitization ratios were achieved for 90 kVp irradiation than 6 MV irradiation. When 5 nM Glu-GNPs were subject to irradiation doses of 2.5, 5, 10, 15, and 20 Gy, the inhibitory rates were 4.23%, 12.6%, 37.5%, 83.75%, and 100%, respectively.

3.5. Intracellular reactive oxygen species (ROS) concentration

To investigate the effect of x-ray induced ROS on cancer cells, we used CM-H2-DCFDA, a fluorescence-based probe that detects the intracellular production of ROS. CM-H2-DCFDA passively diffuses into cells, and becomes deacetylated by intracellular esterases. It is subsequently oxidized to a fluorescent product in the presence of intracellular ROS where the fluorescence indicates the level of intracellular oxidative stress. Figure 3 showed that Glu-GNPs enhance the production of intracellular ROS when irradiated with 8 Gy x-rays. 90 kVp irradiations at 8 Gy induced an approximately 5.1-fold increase in basal CM-H2-DCFDA fluorescence (figure 3(C)), which was enhanced to an 8.3-fold increase by adding 5 nM Glu-GNPs before x-irradiation ($p < 0.05$) (figure 3(D)). Similarly, 6 MV irradiation at 8 Gy induced a 3.4-fold increase for irradiation alone and a 7.8-fold increase for irradiation plus GNPs in basal CM-H2-DCFDA fluorescence ($p < 0.05$) (figures 3(E) and (F)).

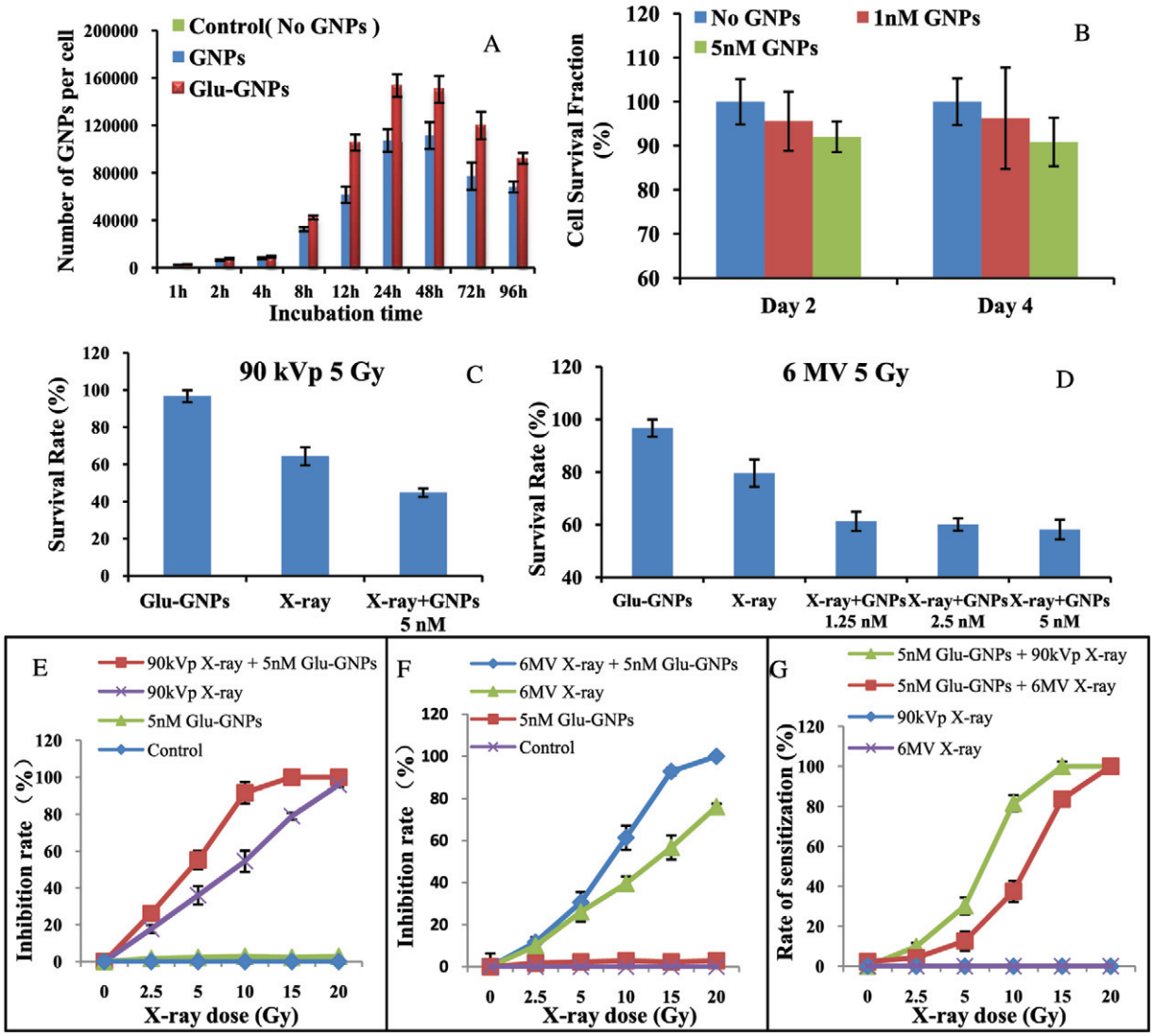

Figure 2. Study of the interactions between nanoparticles and SK-OV-3 cells. After culturing with either GNPs or Glu-GNPs for 24 h, SK-OV-3 cancer cells were used for analyzing the uptake and cytotoxicity effects of nanoparticles, or for treating by the irradiation (5 Gy): (A) cell uptakes of GNPs versus Glu-GNPs; (B) cytotoxicity induced by GNPs and Glu-GNPs measured by the MTT assay; (C) survival rates for groups with 90 kVp irradiation (5 Gy) plus Glu-GNPs measured by the MTT assay; (D) survival rates for groups with 6 MV irradiation (5 Gy) plus Glu-GNPs measured by the MTT assay. GNPs enhanced radiotherapy measured by the colony formation: the inhibition rate induced by Glu-GNPs plus different doses of 90 kVp irradiation (E) or 6 MV irradiation (F); (G) comparison of the enhancement of using GNPs with either 90 kVp irradiation or 6 MV irradiation.

3.6. Apoptosis detection by flow cytometry

To assess the effect of GNPs on 6 MV x-ray induced apoptosis, dual staining of cells with Annexin V-FITC and PI was used to quantitatively distinguish apoptotic cells from normal and necrotic cells. Dots in the lower-right (LR) quadrant represent early stage apoptotic cells and dots in the upper-right (UR) quadrant represent late stage apoptotic cells. Therefore, the sum of LR and UR represents the apoptotic rate. Before irradiation, cells in the Glu-GNP group experienced similar levels of apoptosis to the control group ($9.26 \pm 2.16\%$ versus $7.06 \pm 2.49\%$, $P = 0.13$). However, exposure to 6 MV irradiation caused significant increases in the apoptosis of SK-OV-3 cells compared to controls ($14.35 \pm 0.90\%$ versus $7.06 \pm 2.49\%$, $P = 0.017$). Glu-GNPs subject to 6 MV irradiation induced a significant increase in apoptosis ($18.57 \pm 1.44\%$) compared to irradiation alone ($14.35 \pm 0.90\%$, $P = 0.003$) (figure 4). These data indicate that one mechanism of the radio enhancement effect of GNPs is due to increased cell apoptosis.

3.7. Glu-GNPs alter cell cycle distribution

Treatment of SK-OV-3 cells with 5 nM Glu-GNP for 2 h induced an increase of cells in the G2/M phase and a decrease of cells in the G0/G1 phase when compared with the control cells (figures 4(F)–(H)). GNPs arrested cells at G2/M, the radiosensitive phases of the cell cycle, and thereby enhanced the radiation sensitivity of SK-OV-3 cells. In this study, 9.28% of the untreated control cells were in the G2/M phase, and Glu-GNP increased the fraction of cells in the G2/M phase

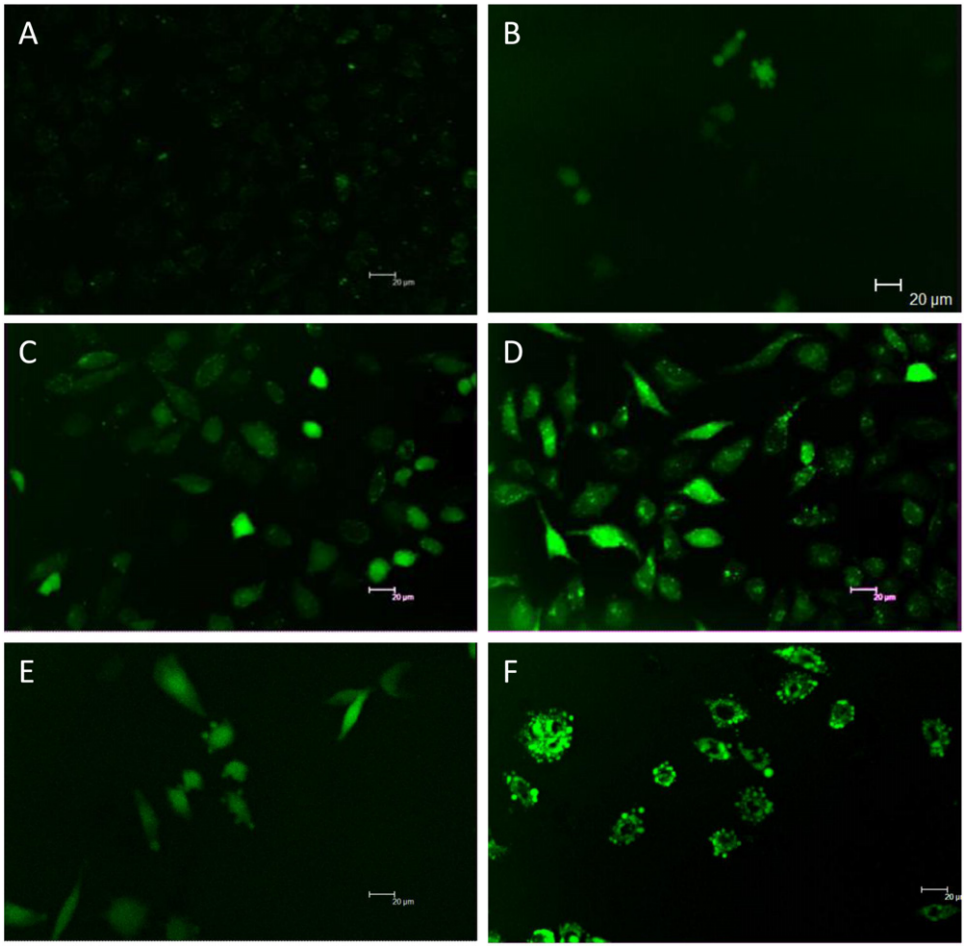

Figure 3. The cellular fluorescence changes resulting from intracellular ROS production were measured by a confocal microscope. After culturing with or without Glu-GNPs for 24 h, SK-OV-3 cancer cells were treated with irradiation:. (A) control; (B) 5 nM Glu-GNPs; (C) 90 kVp irradiation (8 Gy); (D) 90 kVp irradiation (8 Gy) + 5 nM Glu-GNPs; (E) 6 MV irradiation (8 Gy), and (F) 6 MV irradiation (8 Gy) + 5 nM Glu-GNPs.

to 20.52%. For the G0/G1 phase, 43.35% for the control was decreased to 27.82% for the cells treated with Glu-GNPs (5 nM) for 2 h.

4. Discussion

Radiation enhancement by metallic nanoparticles has been widely reported both *in vivo* [7] and *in vitro* [8–11]. In animal testing, GNPs significantly increased the survival rate of mice bearing subcutaneous EMT-6 mammary carcinomas after receiving 250 kVp x-rays [7]. Meanwhile, Rahman *et al* reported the radiation enhancing effects of kilovoltage x-rays and megavoltage electrons in bovine endothelial cells [9]. Our previous study showed that the radiation efficiency of 200 kVp x-rays significantly increased for breast cancer and prostate cancer cells containing internalized Glu-GNPs [12, 13]. Our experiments are the first worldwide to demonstrate that Glu-GNPs enhance the sensitivity of ovarian cancer cells to 6 MV photons and 90 kVp x-rays.

A major engineering challenge is the delivery of nanoparticles to the targeted tumor site. Various approaches for targeted delivery have been investigated [15, 16]. Our experiments used glucose as a targeting ligand to coat the surface of GNPs. Since cancerous cells metabolize much faster, they uptake glucose at significantly higher rates, allowing for selective internalization of Glu-GNPs [12]. The faster cancer cells grow, the faster the metabolism rate, and thus the more uptake of glucose. It is difficult to accurately make the comparison between cells' uptake of Glu-GNPs by ovarian cancer cells and by normal ovarian cells using *in vitro* tests because *in vitro* tests cannot properly present the growth rate of the normal ovarian cells. However, our *in vivo* data indicated that the biodistribution of Glu-GNPs in cancer tissue is ten times higher than those in normal ovarian and uterus tissue (unpublished data) (see supporting data available at stacks.iop.org/Nano/22/285101/mmedia). In this study, uptake concentrations reached peak levels between 24 and 48 h, then diminished thereafter. Glucose significantly increased the localized uptake of GNPs by SK-OV-3 cells and, moreover, allowed nanoparticles to stay internalized longer in the cytoplasm. Based on observed cell uptake kinetics, a radiotherapy regimen was formulated to administer irradiation 24 h after GNPs were injected into the bloodstream.

In developing GNP enhanced radiotherapy, most studies have focused on low-energy radiation because high atomic

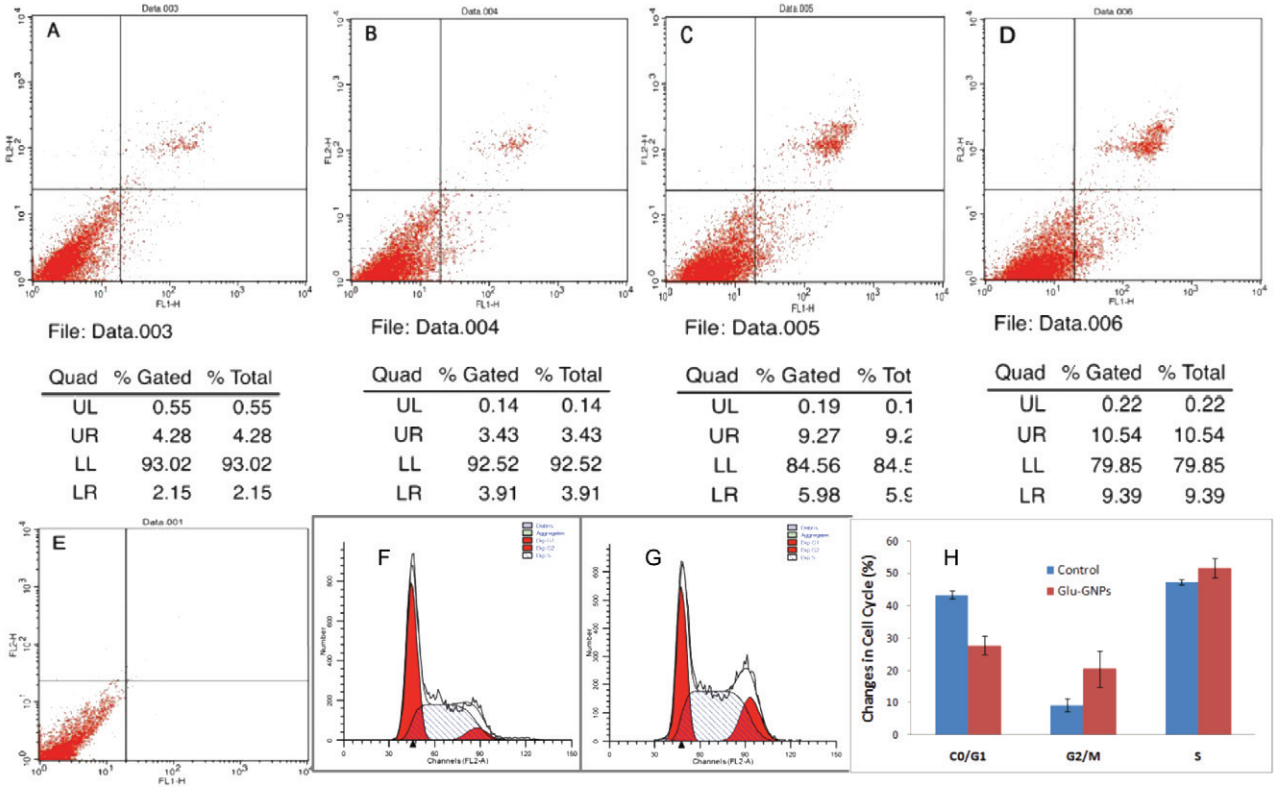

Figure 4. The cell apoptosis induced by Glu-GNPs induced radiotherapy was measured by the flow cytometry dot plots of Annexin V-FITC/PI dual staining. After culturing with or without Glu-GNPs for 24 h, SK-OV-3 cancer cells were detected by flow cytometry: (A) control, (B) Glu-GNPs alone, (C) x-ray alone, (D) Glu-GNPs + x-ray, (E) blank. The flow cytometric analysis of the cell cycle induced by Glu-GNPs: (F) control without treatment; (G) treatment with Glu-GNPs; and (H) comparison of the changes of cell cycle between the control group and the cells treated with Glu-GNPs for 2 h.

number (Z) materials such as gold preferentially absorb kilovoltage x-rays compared to higher-energy megavoltage radiation [17]. Our present study demonstrates that Glu-GNPs achieved superior enhancement ratios at 90 kVp than 6 MV. However, orthovoltage x-rays are limited in therapeutic applications, only effective for cancer near the body's surface. Megavoltage x-rays are far more common in radiotherapy, particularly for deep-seated tumors such as ovarian cancer. Hence, for radio-therapeutic treatment of ovarian cancer it seems far more practical to use GNPs to enhance megavoltage radiotherapy. Data in figures 2(D) and 4(F) show that Glu-GNPs enhance radiation sensitivity toward 6 MV photons by 24% in SK-OV-3 cells. The effect of amplified MV x-rays on cell apoptosis cannot be singularly attributed to high-Z materials alone, additional mechanisms must be considered, such as GNP interactions with the cellular cycle [18].

Ionizing radiation is known to generate ·OH radicals through radiolysis of water molecules. These free radicals react rapidly with multitudes of biological macromolecules, such as nucleic acids, proteins, and lipids to induce nucleic base damage, DNA–protein cross-links, lipid peroxidation, and protein degradation [17, 20]. These factors are a potential trigger for radiation-induced apoptosis [21, 22]. Although GNPs alone at a very high concentration (10 μM) were reported to generate a significant level of ROS [19], this concentration is too high for clinical applications. In the present study, to our knowledge, we are the first group to demonstrate that Glu-GNPs at very low concentration (5 nM) with 6 MV x-ray irradiation can produce a high level of intracellular ROS to kill ovarian cancer cells (figure 3). These ROS lead to higher elevated levels of oxidative stress manifesting as increased levels of apoptosis compared to irradiation alone (figure 4). The results indicate that increased ROS formation when radiation interacts with GNPs is a key mechanism that mediates cancer cell apoptosis.

Another intriguing aspect of GNPs' behavior is their disproportionate cytotoxicity toward cancer cells. In our previous study, MCF-7 cancer cells and MCF-10A normal cells (non-cancerous) were made to internalize the same concentration of GNPs with the expectation that they would induce similar irradiation cytotoxicities [12]. However, after being exposed to identical radiation doses, the viability of the cancer cells decreased significantly (about 40%) while no significant changes were observed in the normal cells [13]. These results provide convincing evidence that GNPs are involved in cellular mechanisms apart from ROS enhancement. Turner *et al* reported that metallic materials may arrest cells at the G2/M phase, the most radiosensitive phase of the cell cycle [23], and thus disproportionately increase the sensitivity of cancer cells toward radiation. Zhang *et al* reported that Glu-GNPs trigger activation of the CDK kinases, leading cancer cells to accumulate in the G2/M phase. Consequently, after

treatment with Glu-GNPs, cancer cells were more sensitive to radiotherapy.

In summary, we demonstrate that Glu-GNPs have remarkable potential to enhance radiotherapy on ovarian cancer cells. Except for kVp irradiation reported previously in [12, 13], the results of our *in vitro* tests on SK-OV-3 cells also showed that Glu-GNPs can significantly increase the cytotoxicity using 6 MV irradiation. We also reported that GNPs, even at very low concentration (5 nM), combined with x-ray irradiation can generate a significant increased ROS production compared to x-rays alone in killing ovarian cancer cells. Furthermore, we hypothesize that GNPs manipulate the cancer cell cycle to increase radiation susceptibility. Our future work will investigate the molecular mechanisms governing GNP enhancement of radiation cytotoxicity, followed by testing the functionalized GNPs in animal models.

Acknowledgments

This project was supported by the grants to Beihua Kong (no. 30872738) and Kun Song (no. 30700897) from the National Natural Science Foundation of China. The project was also supported by grants from the National Research Council/National Institute of Nanotechnology, Canada and the Canadian Cancer Research Alliance.

References

[1] Gubbels J A *et al* 2010 The detection, treatment, and biology of epithelial ovarian cancer *J. Ovarian Res.* **3** 8
[2] Jemal A *et al* 2009 Cancer statistics, 2009 *CA Cancer J. Clin.* **59** 225–49
[3] Chobanian N and Dietrich C S III 2008 Ovarian cancer *Surg. Clin. North Am.* **88** 285–99
[4] Kawasaki E S and Player A 2005 Nanotechnology, nanomedicine, and the development of new, effective therapies for cancer *Nanomedicine* **1** 101–9
[5] Wang C H *et al* 2007 Structural properties of naked gold nanoparticles formed bysynchrotron x-ray irradiation *J. Synchrotron Radiat.* **14** 477–82
[6] Herold D M *et al* 2000 Gold microspheres: a selective technique for producing biologically effective dose enhancement *Int. J. Radiat. Biol.* **76** 1357–64
[7] Hainfeld J F, Slatkin D N and Smilowitz H M 2004 The use of gold nanoparticles to enhance radiotherapy in mice *Phys. Med. Biol.* **49** N309–15
[8] Hainfeld J F *et al* 2008 Radiotherapy enhancement with gold nanoparticles *J. Pharm. Pharmacol.* **60** 977–85
[9] Rahman W N *et al* 2009 Enhancement of radiation effects by gold nanoparticles for superficial radiation therapy *Nanomedicine* **5** 136–42
[10] Chithrani D B *et al* 2010 Gold nanoparticles as radiation sensitizers in cancer therapy *Radiat. Res.* **173** 719–28
[11] Liu C J *et al* 2010 Enhancement of cell radiation sensitivity by pegylated gold nanoparticles *Phys. Med. Biol.* **55** 931–45
[12] Kong T *et al* 2008 Enhancement of radiation cytotoxicity in breast-cancer cells by localized attachment of gold nanoparticles *Small* **4** 1537–43
[13] Zhang X *et al* 2008 Enhanced radiation sensitivity in prostate cancer by gold-nanoparticles *Clin. Invest. Med.* **31** E160–7
[14] Tian Y Y, An L J, Jiang L, Duan Y L, Chen J and Jiang B 2006 Catalpol protects dopaminergic neurons from LPS-induced neurotoxicity in mesencephalic neuron-glia cultures *Life Sci.* **80** 193–9
[15] Lee S *et al* 2007 Biological imaging of HEK293 cells expressing PLCgamma1 using surface-enhanced Raman microscopy *Anal. Chem.* **79** 916–22
[16] Huang X *et al* 2006 Cancer cell imaging and photothermal therapy in the near-infrared region by using gold nanorods *J. Am. Chem. Soc.* **128** 2115–20
[17] Dizdaroglu M 1991 Chemical determination of free radical-induced damage to DNA *Free Radic. Biol. Med.* **10** 225–42
[18] Roa W *et al* 2009 Gold nanoparticle sensitize radiotherapy of prostate cancer cells by regulation of the cell cycle *Nanotechnology* **20** 375101
[19] Chompoosor A *et al* 2010 The role of surface functionality on acute cytotoxicity, ROS generation and DNA damage by cationic gold nanoparticles *Small* **6** 2246–9
[20] Riley P A 1994 Free radicals in biology: oxidative stress and the effects of ionizing radiation *Int. J. Radiat. Biol.* **65** 27–33
[21] Kolesnick R and Fuks Z 2003 Radiation and ceramide-induced apoptosis *Oncogene* **22** 5897–906
[22] Ojeda F, Diehl H A and Folch H 1994 Radiation induced membrane changes and programmed cell death: possible interrelationships *Scanning Microsc.* **3** 645–51
[23] Turner J *et al* 2005 Tachpyridine, a metal chelator, induces G2 cell-cycle arrest, activates checkpoint kinases, and sensitizes cells to ionizing radiation *Blood* **106** 3191–9